ACS OMEGA

Open Access

This article is licensed under CC-BY-NC-ND 4.0

http://pubs.acs.org/journal/acsodf

Article

Design and Biological Evaluation of Palladium(II)−Phosphine−Benzimidazole Complexes as Dual Antioxidant and Antiangiogenic Agents

Hülya Tuba Kiyan, Kübra Ögüt,* Pervin Soyer, Hakan Ünver, and Deniz Erol Kutucu

Cite This: https://doi.org/10.1021/acsomega.5c04508

Read Online

ACCESS | Metrics & More | Article Recommendations | Supporting Information

ABSTRACT: The present study describes the design, synthesis, and characterization of two novel palladium(II) complexes incorporating phosphine and benzimidazole ligands, followed by a comprehensive evaluation of their antioxidant and antiangiogenic properties. The complexes were fully characterized using spectroscopic and analytical methods. Antioxidant capacity was investigated through a multiassay approach, including ferrous ion-chelating activity, reducing power, and $ABTS^{\bullet+}$ radical cation decolorization. Antiangiogenic activity was evaluated *in vivo* using the chick chorioallantoic membrane (CAM) assay. Palladium complex 1 exhibited the strongest ferrous ion-chelating ability (71.91% inhibition) and the highest $ABTS^{\bullet+}$ scavenging activity (49.79%), while Palladium complex 2 demonstrated superior reducing power (EC_{50} = 1.06 mg/mL). Both complexes showed strong antiangiogenic effects, with Palladium complex 1 achieving an average inhibition score of 0.90—comparable to the positive control (±)-thalidomide—and without observable irritation or toxicity. These results indicate that both complexes possess potent biological activities; however, the overall antioxidant and antiangiogenic profile of Palladium complex 1 suggests it may be particularly promising as a redox-modulating agent targeting oxidative stress−induced angiogenesis. To the best of our knowledge, this is the first report of palladium−phosphine−benzimidazole complexes demonstrating such dual activity, highlighting their potential as multifunctional candidates in cancer-related therapeutic research.

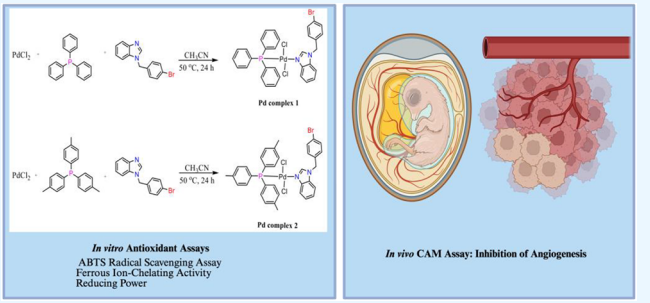

1. INTRODUCTION

Angiogenesis, the physiological process of new blood vessel formation, plays a critical role in wound healing, embryonic development, and reproductive functions. However, dysregulated angiogenesis is closely associated with a range of pathological conditions, including cancer, atherosclerosis, rheumatoid arthritis, diabetic retinopathy, and psoriasis.[1,2] Antiangiogenesis therapy, which uses active substances that either stop the vascularization necessary to maintain the tumor or compromise the function of current blood vessels, is the principal area of study on attacking the tumor microenvironment. Angioprevention has also attracted a lot of interest as a technique to find novel cancer treatment strategies using antitumor medications with high antiangiogenic potential at low doses and lower toxicity.[3,4] The chick chorioallantoic membrane (CAM) assay is a widely accepted *in vivo* model for evaluating the angiogenic or antiangiogenic potential of pharmacological compounds. The CAM model enables the investigation of vascular development, tumor growth, tissue grafting, and drug delivery while offering significant advantages such as low cost, rapid results, and exemption from ethical approval required for vertebrate animal studies. Furthermore, since the model is applied during early embryonic development (typically between days 3 and 7), it provides a suitable and ethically favorable alternative to classical animal experiments.[5]

Metal-based complexes, particularly those incorporating platinum(II) and palladium(II), have played a crucial role in the development of chemotherapeutic agents and continue to inspire the design of new anticancer frameworks.[6] Palladium(II) complexes are notably appealing in medicinal chemistry owing to their superior ligand exchange rates relative to platinum counterparts, facilitating enhanced structural flexibility and adaptability in drug design.[7−9] Unlike platinum(II) molecules, which frequently demonstrate inadequate selectivity and elevated toxicity, Pd(II) complexes display superior kinetic characteristics, reduced toxicity, and heightened reactivity toward biological targets.[10] Moreover, Pd(II) centers easily adopt square-planar geometries, rendering them suitable for

Received: May 14, 2025
Revised: August 6, 2025
Accepted: August 19, 2025

Downloaded via 176.54.211.78 on December 4, 2025 at 19:33:43 (UTC).
See https://pubs.acs.org/sharingguidelines for options on how to legitimately share published articles.

© XXXX The Authors. Published by American Chemical Society

the construction of targeted agents with predictable coordination environments, essential for biological interactions.[11,12]

In recent decades, palladium-based metal complexes have attracted considerable attention in anticancer drug development due to their ability to mimic platinum(II) compounds while offering enhanced reactivity and potentially lower toxicity.[13] Recent studies emphasize that palladium systems can be more readily modified to improve selectivity, reduce systemic toxicity, and enhance pharmacokinetic profiles, which are critical parameters in anticancer therapy. These features make them attractive scaffolds for the design of multifunctional drug candidates with both cytotoxic and antiangiogenic potential.[14,15] Moreover, palladium(II) complexes have been reported to exhibit effective DNA-binding affinity, selective cytotoxicity toward cancer cells, and reduced nephrotoxicity compared to platinum analogs, particularly cisplatin. These characteristics make palladium-based scaffolds not only structurally versatile but also biologically favorable for the development of novel chemotherapeutic agents.[16−18]

Palladium(II) complexes were chosen for this study because of their structural similarity to platinum(II) compounds and improved kinetic lability, which allows for greater flexibility in ligand exchange in biological environments.[19−21] In redox-sensitive systems, this characteristic enables quick contact with biomolecular targets, which may increase pharmacodynamic efficiency.[22] Moreover, Pd(II)-based systems provide a chance to create metal complexes with adjustable electrical and geometric characteristics, which would allow for the creation of multipurpose scaffolds with anticancer, antioxidant, and antiangiogenic potential.[23−26] Palladium II has greater modifiability and lower intrinsic toxicity than platinum II, which makes it a desirable substitute in the hunt for metal-based medicinal agents.[23−25] Additionally, the redox-active nature of palladium(II) may result in undesired interactions with biological molecules, leading to off-target effects or increased toxicity in complex biological environments.[27] The biological relevance of palladium coordination compounds has been particularly noted in the context of DNA binding, enzyme inhibition, and redox modulation—properties that are critical for anticancer activity.[28,29] Along with the central metal ion, the choice of ancillary ligands plays a critical role in determining the pharmacological behavior of metal complexes. Phosphine ligands, widely utilized in coordination chemistry, contribute significantly to the stability, lipophilicity, and biological targeting of metal complexes. Numerous phosphine-containing metal complexes, including those of gold and ruthenium, have shown potent anticancer activity and modulation of antioxidant enzymes, particularly in leukemia and lung cancer models.[30−32] In parallel, benzimidazole-based scaffolds continue to attract attention due to their diverse pharmacological activities. Compounds bearing benzimidazole rings have been reported to exhibit a wide range of bioactivities, including anticancer, antimicrobial, antidiabetic, antiviral, and anti-inflammatory properties.[33,34] The structural resemblance of benzimidazole to nucleobases and enzyme substrates underlies its biological efficacy, making it an attractive pharmacophore in drug design.[35]

Motivated by the complementary biological relevance of phosphine and benzimidazole ligands, the present study focuses on the design, synthesis, and characterization of two novel palladium(II) complexes incorporating both ligand types. The structural features of the synthesized complexes were confirmed through spectroscopic and analytical techniques. Their antioxidant potential was evaluated using the ABTS radical cation decolorization assay, while antiangiogenic activity was assessed *in vivo* via the chick chorioallantoic membrane (CAM) assay, a widely accepted and ethically favorable model for the preliminary screening of angiogenesis modulators.[32−38] However, despite their promising pharmacological properties, palladium-based complexes also present certain limitations that must be addressed for their successful therapeutic application. One of the primary challenges is their higher kinetic lability compared to platinum analogs, which can lead to premature ligand dissociation under physiological conditions, potentially affecting both selectivity and stability.[29,39] Moreover, limited *in vivo* studies and scarce clinical translation of palladium-based candidates highlight the need for further investigation into their bioavailability, metabolic stability, and long-term safety profiles.[40] Despite there is increasing interest in palladium(II) complexes as prospective anticancer treatments, the majority of research thus far concentrates exclusively on cytotoxicity or DNA-binding affinity, neglecting a comprehensive assessment of their antioxidant and antiangiogenic effects concurrently.[41] Moreover, research frequently lacks intentional modifications in ligand design to clarify structure−activity correlations. For instance, whereas Pd-based systems exhibit promising biological effects, there is insufficient investigation into the impact of electrically adjustable phosphine-benzimidazole ligands on dual bioactivity.[42] This study fills these gaps by synthesizing Pd(II) complexes with electronic substituents in the benzimidazole moiety and assessing their multifunctional antioxidant and antiangiogenic properties in both *in vitro* and *in vivo* scenarios.[43]

In this study, two novel palladium(II) complexes incorporating both phosphine and benzimidazole ligands were synthesized and structurally characterized using various spectroscopic techniques. Their antioxidant potential was evaluated through a multiassay approach, including ferrous ion-chelating activity, reducing power measurement, and $ABTS^{\bullet+}$ radical cation decolorization. This comprehensive *in vitro* assessment provides a more robust understanding of their redox-modulating capabilities. In parallel, their antiangiogenic activity was assessed *in vivo* via the chick chorioallantoic membrane (CAM) assay, a widely accepted and ethically favorable model for the preliminary screening of angiogenesis modulators. To the best of our knowledge, this is the first study to report palladium(II) complexes bearing both phosphine and electronically modulated benzimidazole ligands that were evaluated using a dual biological screening strategy. The combination of a structurally tunable ligand system with integrated antioxidant and antiangiogenic assays provides new insights into the design of multifunctional metal-based therapeutics. Our approach emphasizes not only the structural adaptability of palladium scaffolds but also their potential in addressing oxidative stress−mediated angiogenesis, a key feature in various cancer pathologies.

2. MATERIALS AND METHODS

2.1. Materials. Oxidized squalene (OSE) was kindly donated by Neutec Pharma Inc. (Istanbul, Türkiye). Poly(lactic-*co*-glycolic acid) (PLGA; 50:50 lactide:glycolide ratio, Mw: 30−60 kDa) and acetone were obtained from Sigma-Aldrich (Berlin, Germany). Poly(ethylene glycol) (PEG 2000) was purchased from Merck (Darmstadt, Germany). Trolox (6-hydroxy-2,5,7,8-tetramethylchroman-2-carboxylic acid) and

https://doi.org/10.1021/acsomega.5c04508
ACS Omega XXXX, XXX, XXX−XXX

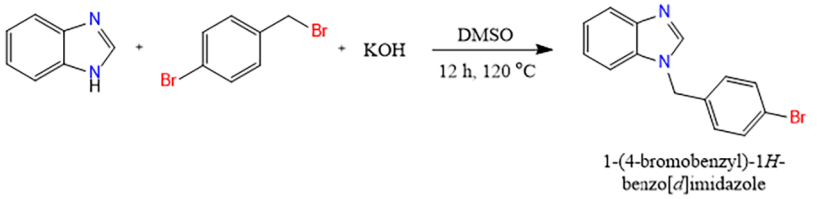

Figure 1. Synthesis reaction of benzimidazole ligand.

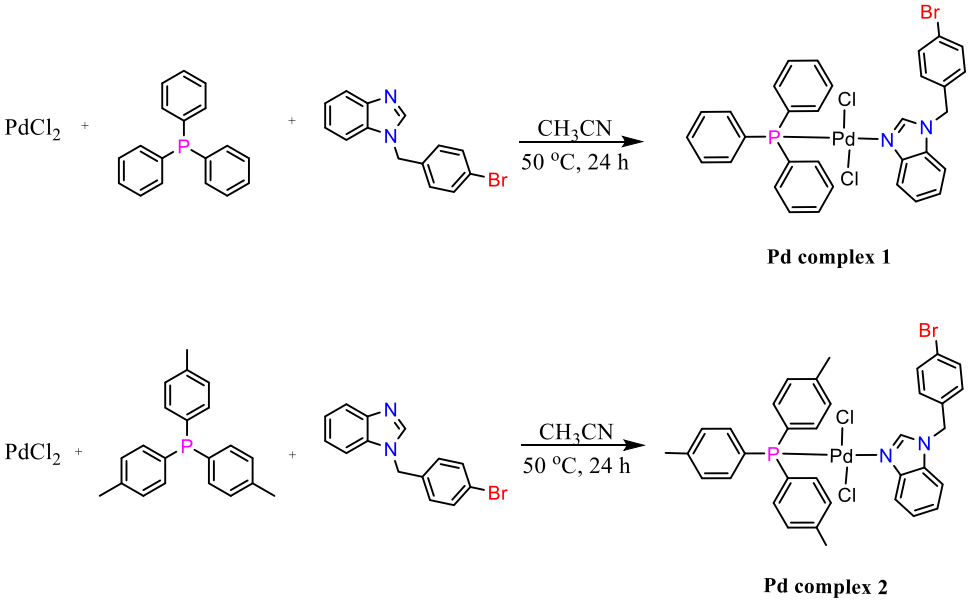

Figure 2. Synthesis scheme of palladium(II) complexes.

ascorbic acid, used as antioxidant reference standards, were also obtained from Sigma-Aldrich. Milli-Q ultrapure water (Millipore, Mosheim, France) was used for all reagent preparations and dilutions. Melting points are determined with using Stuart SMP-30 melting point device. Fourier Transform Infrared (FT-IR) spectra were recorded using a PerkinElmer Spectrum 100 FT-IR spectrometer over the range of 4000−400 cm^{-1}. ^{1}H NMR (400 MHz) and ^{13}C NMR (100 MHz) spectra were obtained on an Agilent DD2 NMR spectrometer at the Department of Chemistry, Eskişehir Technical University. Elemental analyses (CHNS/O) of all compounds were carried out using a PerkinElmer 2400 Series II CHNS/O Analyzer. Single-crystal X-ray diffraction data were collected using a Bruker D8 QUEST diffractometer at Scientific and Technological Research Application and Research Center, Sinop University, Türkiye.

The chemicals used in the synthesis and antiangiogenic experiments included palladium(II) chloride (99%), triphenylphosphine (99%), 4-bromobenzyl bromide (99%), hydrazine monohydrate (98%), phenylacetic acid (99%), and sodium hydroxide (>97%), all purchased from Sigma-Aldrich (Germany). Additionally, agarose and sodium dodecyl sulfate (SDS) were obtained from Fluka, and (±)-thalidomide from Sigma-Aldrich. Benzimidazole ligands and palladium(II) complexes were kindly provided by Prof. Dr. Hakan Ünver. Fertilized hen eggs used for CAM assays were supplied by Has Tavuk Company (Bursa and Sivrihisar, Türkiye). All other reagents used in this study were of analytical grade and used without further purification.

2.2. Synthesis. *2.2.1. Synthesis of 1-(4-Bromobenzyl)-1H-benzo[d]imidazole.* 1-(4-Bromobenzyl)-1*H*-benzo[*d*]-imidazole was synthesized via a nucleophilic substitution reaction between benzimidazole and 4-bromobenzyl bromide, as illustrated in Figure 1.

1*H*-Benzimidazole (1.18 g, 0.01 mol) was dissolved in dimethyl sulfoxide (DMSO, 50 mL), followed by the addition of potassium hydroxide (0.61 g, 0.01 mol). The resulting mixture was stirred at 100 °C for 1 h to ensure deprotonation of the benzimidazole. Subsequently, 4-bromobenzyl bromide (2.62 g, 0.011 mol) was added dropwise, and the reaction mixture was refluxed at 120 °C for 12 h. Upon completion, the reaction solvent evaporated and remained material subjected to colum chromatography (EtOAc/Hexane: 1/5) and the pure product obtained as white crystals (1.16 g, 40%).

M.p.: 84−86 °C **Elemental Analysis of $C_{14}H_{11}N_2Br$: Calculated** (%) C = 58.56; H = 3.86; N = 9.76; **Experimental** (%): C = 58.16; H = 4.11; N = 9.32. **FT-IR (KBr) cm^{-1}**: 3077−2932, 1488, 1459, 1364, 1285, 1260, 740. **^{1}H NMR (400 MHz, DMSO-d^6)**: δ (ppm) 8.41 (s, 1H), 7.65 (d, J = 6.5 Hz, 1H), 7.58−7.44 (m, 3H), 7.22 (dd, J = 24.0, 6.5 Hz, 4H), 5.48 (s, 2H). **^{13}C NMR (100 MHz, DMSO-d^6)**: δ (ppm) 136.90, 132.08, 130.08, 122.93, 122.12, 121.36, 120.01, 111.13, 47.37, 39.96.

2.2.2. Synthesis of Palladium(II) Complexes. The palladium(II) complexes were synthesized via a stepwise coordination strategy, as illustrated in Figure 2. Initially, triphenylphosphine (for Complex 1) or trip-tolylphosphine (for Complex 2) (3 mmol). was dissolved in 20 mL of acetonitrile and added dropwise to a separate solution of

https://doi.org/10.1021/acsomega.5c04508
ACS Omega XXXX, XXX, XXX−XXX

palladium(II) chloride (530 mg, 3 mmol) also prepared in 20 mL of acetonitrile. The mixture was stirred at 50 °C for 1 h using a magnetic hot plate to facilitate the precoordination of the phosphine ligands to the palladium center. Following this, the previously synthesized benzimidazole ligand (860 mg, 3 mmol). was introduced dropwise into the reaction mixture. The resulting solution was stirred under the same conditions (50 °C) for an additional 24 h to ensure complete coordination. Upon completion of the reaction, the solvent was allowed to evaporate slowly at room temperature, leading to the formation of crystalline palladium(II) complexes.

Palladium complex 1: (1.05 g, 48%). **M.p.**: 222−224 °C **Elemental Analysis of $C_{32}H_{26}BrCl_2N_2PPd$: Calculated** (%): C, 52.88; H, 3.61; N, 3.85, **Experimental** (%): C, 52.75; H, 3.42; N, 3.83. **FT-IR (KBr) cm^{-1}**: 3082−2837, 1592, 1498, 1290, 1251, 1178, 1099, 1021, 825, 799, 752, 727, 537. **^{1}H NMR (400 MHz, DMSO-d6): δ (ppm)** 8.71 (s, 1H), 7.81−7.68 (m, 4H), 7.63−7.43 (m, 13H), 7.32 (s, 6H), 5.58 (s, 2H). **^{13}C NMR (100 MHz, DMSO-d6): δ (ppm)** 134.93, 134.83, 134.47, 134.37, 132.20, 131.57, 130.65, 130.41, 129.90, 128.79, 128.68, 112.13, 48.11, 39.96.

Palladium complex 2: (1.25 g, 54%). **M.p.**: 235−237 °C **Elemental Analysis of $C_{35}H_{32}BrCl_2N_2PPd$: Calculated** (%): C, 54.68; H, 4.20; N, 3.64: **Experimental** (%) C, 54.18; H, 4.35; N, 3.16. **FT-IR (KBr) cm^{-1}**: 3104−2837, 1592, 1520, 1489, 1463, 1390, 1261, 1188, 752. **^{1}H NMR (400 MHz, DMSO-d6): δ (ppm)** 8.73 (s, 1H), 7.57 (d, J = 7.9 Hz, 6H), 7.44 (d, J = 9.0 Hz, 2H), 7.30 (d, J = 6.6 Hz, 9H), 7.07 (s, 3H), 5.58 (s, 2H), 2.34 (s, 9H). **^{13}C NMR (100 MHz, DMSO-d6): δ (ppm)** 141.42, 134.82, 134.72, 134.34, 134.23, 132.20, 130.86, 130.40, 129.34, 129.22, 111.96, 48.19, 39.96, 21.46.

2.2.3. Characterization of Synthesized Compounds. The structural and physicochemical properties of the synthesized compounds were verified through a combination of analytical and spectroscopic techniques. These primarily included single-crystal X-ray diffraction (SC-XRD), nuclear magnetic resonance spectroscopy (^{1}H and ^{13}C NMR), Fourier-transform infrared spectroscopy (FT-IR), and elemental analysis.

2.2.4. Crystallographic Studies. Single-crystal X-ray diffraction data were collected at 297.11 K using a Bruker D8 QUEST diffractometer equipped with a rotating anode and graphite-monochromated Mo Kα radiation (λ = 0.71073 Å). The collected data were processed using the Bruker SMART software package.[44] Structure determination was carried out with Olex2[45] and refinement was performed by least-squares methods using SHELXL.[46] All non-hydrogen atoms were refined with anisotropic displacement parameters, while hydrogen atoms were positioned geometrically and refined using a riding model. Structural visualization and analysis of geometric parameters were conducted with the MERCURY software.[47] The crystallographic information has been deposited in the Cambridge Crystallographic Data Centre.

2.3. Biological Activity. *2.3.1. In Vitro Ferrous Ion-Chelating Activity.* The ferrous ion-chelating activity of the test compounds was evaluated using a previously described method with slight modifications.[48,49] Briefly, 400 μL of each sample solution was mixed with 740 μL of methanol and 40 μL of $FeCl_2$ solution (2 mM). The reaction was initiated by adding 80 μL of ferrozine solution (5 mM). The mixture was incubated at room temperature for 10 min, and the absorbance was recorded at 562 nm using a microplate reader. The percentage inhibition of ferrozine−Fe^{2+} complex formation was calculated using the following equation

$$\%\mathrm{Inh} = \left(\frac{\mathrm{Abs}_{\mathrm{blank}} - \mathrm{Abs}_{\mathrm{sample}}}{\mathrm{Abs}_{\mathrm{blank}}}\right) \times 100$$

where $\mathrm{Abs}_{\mathrm{blank}}$ is the absorbance of the control (containing $FeCl_2$ and ferrozine without sample), and $\mathrm{Abs}_{\mathrm{sample}}$ is the absorbance in the presence of the test sample. All analyses were performed in duplicate, and the results were expressed as mean ± standard error of the mean (S.E.M).[50]

2.3.2. In Vitro Reducing Power. The reducing power of the samples was evaluated based on the method described, with slight modifications.[51,52] Briefly, 200 μL of each sample was mixed with 2.5 mL of either water or ethanol, 200 mM sodium phosphate buffer (pH 6.6), and 1% potassium ferricyanide solution. The reaction mixture was incubated at 50 °C for 20 min. After incubation, 500 μL of 10% (w/v) trichloroacetic acid was added to terminate the reaction, followed by centrifugation at 4000g for 10 minutes. Next, 500 μL of the supernatant was combined with 500 μL of 0.1% ferric chloride solution and 200 μL of deionized water. The absorbance was measured at 700 nm against a blank. An increase in absorbance indicated enhanced reducing power.

The effective concentration (EC_{50}; mg/mL) at which the absorbance reached a value of 0.5 was determined using linear regression analysis. For comparison, ascorbic acid, butylated hydroxyanisole (BHA), and tocopherol were used as reference antioxidants.[53]

2.3.3. Trolox Equivalent Antioxidant Activity (TEAC). The antioxidant capacity of the synthesized compounds was evaluated using the $ABTS^{\bullet+}$ radical cation decolorization assay, with slight modifications.[54,55] A 7 mM ABTS stock solution was prepared by reacting ABTS with 2.45 mM potassium persulfate in distilled water. The mixture was incubated in the dark at room temperature for 12−16 hours to generate the $ABTS^{\bullet+}$ radical cation. Prior to use, the resulting solution was diluted with absolute ethanol to achieve an absorbance of 0.700 ± 0.02 at 734 nm. For the assay, 10 μL of each test sample (at a concentration of 0.5 mg/mL in ethanol) was added to 990 μL of the $ABTS^{\bullet+}$ working solution. The mixture was incubated for 5 minutes in the dark, and the absorbance was then measured at 734 nm using a microplate reader. Ethanol was used as the blank, and Trolox (0.5 mg/mL in ethanol) served as the positive control. The percentage of radical scavenging activity (RSA) was calculated using the following formula

$$\%\mathrm{Inh} = \left(\frac{\mathrm{Abs}_{\mathrm{control}} - \mathrm{Abs}_{\mathrm{sample}}}{\mathrm{Abs}_{\mathrm{control}}}\right) \times 100$$

All assays were performed in triplicate, and the results were expressed as mean percentage inhibition ± standard error of the mean (SEM). SigmaPlot software (version 15.0) was used for data analysis and graphing.

2.4. *In Vivo* Angiogenic Activity (CAM Assay). *2.4.1. Preparation of Test Samples for CAM Assay.* Benzimidazole derivatives and newly synthesized palladium complexes (0.5−5 mg/mL), along with a positive control ((±)-thalidomide, 5 mg/mL) and a negative control (sodium dodecyl sulfate, SDS, 5 mg/mL), were dissolved in a 2.5% (w/v) agarose solution. Each solution (10 μL) was carefully dropped onto 5 mm diameter circular stainless-steel supports

https://doi.org/10.1021/acsomega.5c04508
ACS Omega XXXX, XXX, XXX−XXX

and allowed to cool at room temperature for complete solidification. The resulting pellets were then applied to the surface of the chick chorioallantoic membrane (CAM) for *in vivo* evaluation.[56,57]

2.4.2. In Vivo Chorioallantoic Membrane (CAM) Assay. The antiangiogenic effects of the synthesized benzimidazole derivatives and palladium(II) complexes were evaluated using the chick embryo chorioallantoic membrane (CAM) assay, as previously described with modifications.[58−61] Fertilized hen eggs were incubated at 36.5 °C and 80% relative humidity for 72 h. To facilitate CAM exposure, approximately 10−15 mL of albumin was removed from each egg via a small puncture on the blunt end, and a window was carefully created using a sterile scalpel two-thirds from the pointed end. The eggshell fragments were removed, and the openings were sealed with stretch film before continuing incubation for an additional 72 h under the same conditions. Following incubation, solidified agarose pellets (2.5% w/v), containing either the test compounds or control agents, were gently placed on the CAM surface. Each pellet was approximately 5 mm in diameter and prepared as described in the sample preparation section. (±)-Thalidomide (50 mg/pellet) and sodium dodecyl sulfate (SDS) served as the positive and negative controls, respectively, while plain agarose was used as the blank. One pellet was applied per egg. After 24 h of treatment, the eggs were examined under a stereomicroscope to evaluate the extent of capillary disruption.

Each experimental group consisted of 10−15 eggs, and all tests were performed in triplicate with duplicate evaluations. Antiangiogenic activity was assessed based on a semi-quantitative scoring system adapted from Kiyan et al. and Ikitimur-Armutak et al.[60,62] The scoring scale was defined as follows: the antiangiogenic response on the CAM surface was assessed using a semiquantitative grading system, as summarized in Table 1. Each embryo received a single

Table 1. Semi-Quantitative Score System of Anti-Angiogenic Effect on Cam after Treatment

score range	antiangiogenic effect	effects observed on CAM after treatment
<0.5	inactive	no change (normal embryo growth)
05−0.75	weak	no capillary free area. Area with reduced density of capillaries around the pellet not larger than its own area
0.75−1.0	strong	small capillary free area or area with significantly reduced density of capillaries. Effects not larger than double the size of the pellet.
1.0>	very strong	capillary free area around the pellet at least doubles the size of the pellet

treatment pellet, and the extent of capillary disruption was observed 24 h postapplication. Based on the observed vascular changes, samples were assigned to one of four categories: inactive, weak, strong, or very strong antiangiogenic effect. To calculate the mean antiangiogenic score for each test group, the following formula was applied, as previously described in the literatüre.[58,63,64]

$$\text{mean score} = \frac{[\text{no. of eggs(score} > 1) \times 2] + [\text{no. of eggs(score } 0.75{-}1) \times 1]}{\text{total number of eggs evaluated}}$$

As internal controls, (±)-thalidomide (50 mg/pellet) and sodium dodecyl sulfate (SDS, 50 mg/pellet) were used as positive and negative references, respectively. Blank treatments consisted of pellets prepared only with 2.5% (w/v) agarose. Each experimental condition was tested in triplicate, and all evaluations were performed under consistent conditions using a stereomicroscope.

2.5. Statistical and Mathematical Analysis. All statistical analyses were performed using GraphPad Prism version 6.0 (GraphPad Software, San Diego, CA). One-way analysis of variance (ANOVA) was used to assess statistical differences among groups. Tukey's multiple comparison post hoc test was applied to determine significance between individual groups. All results were expressed as mean ± standard deviation (SD). A p-value of less than 0.05 ($p < 0.05$) was considered statistically significant.

3. RESULTS AND DISCUSSION

3.1. Structural Analysis of Benzimidazole ligand. The FT-IR spectra of benzimidazole ligand (Figure S1) exhibited characteristic C−H stretching vibrations in the 3080−2870 cm^{-1} range and distinct aromatic C═C and C═N stretching bands around 1490 and 1360 cm^{-1}, confirming the proposed structure.

In the ^{1}H NMR spectrum of the benzimidazole ligand (Figure S2), a singlet corresponding to the two methylene ($-CH_2-$) protons was observed at 5.48 ppm. The aromatic proton signals appeared within the expected range of 7.19−7.66 ppm. Additionally, a downfield signal at 8.41 ppm was assigned to the CH proton. In the ^{13}C NMR spectrum of the benzimidazole ligand (Figure S3), the methylene ($-CH_2-$) carbon resonance was observed at 47.37 ppm. Aromatic carbon signals appeared in the range of 111.13−132.08 ppm, while the CH carbon signal was detected at 136.90 ppm. These spectral features are consistent with the proposed structure of the ligand.

3.2. Structural Analysis of Palladium(II) Complexes. The FT-IR spectra of palladium complexes 1 and 2 (Figures S4 and S7) exhibited strong absorption bands around 1592 cm^{-1}, attributed to the C═N stretching vibration of the benzimidazole moiety, confirming coordination through the nitrogen atom. Additional bands observed in the 1498−1021 cm^{-1} region are consistent with phosphine and aromatic functionalities. Furthermore, absorptions in the low-frequency range (727−537 cm^{-1}) correspond to metal−ligand vibrational modes. These spectral features provide strong evidence for the successful formation of stable palladium−phosphine−benzimidazole frameworks.

In the ^{1}H NMR spectra of both palladium complexes (Figures S5 and S8), singlet peaks observed at 5.58 ppm is related with methylene ($-CH_2-$) protons. The methylene proton signals observed at 5.48 ppm in the free ligand shifted to 5.58 ppm upon complexation. Aromatic proton signals were detected in the range of 7.07−7.75 ppm for both complexes. Additionally, the CH proton signal, which appeared at 8.41 ppm in the free ligand, shifted to an average of 8.7 ppm after coordination. In the ^{13}C NMR spectrum of the free benzimidazole ligand, the methylene ($-CH_2-$) carbon resonance appears at 47.37 ppm. Upon coordination to palladium, this signal shifts slightly downfield and is observed at approximately 48.15 ppm in both complexes (Figures S6 and S9). Aromatic carbon signals for the complexes are detected in the range of 111.96−134.93 ppm. The CH carbon resonance, initially observed at 136.90 ppm in the free ligand, appears at 145.64 ppm in complex 1 and at 141.42 ppm in

https://doi.org/10.1021/acsomega.5c04508
ACS Omega XXXX, XXX, XXX−XXX

complex 2. These downfield shifts in carbon resonances further confirm the coordination of the ligand to the palladium center and the formation of distinct metal complexes.

3.3. Single Crystal X-ray Analysis. Single crystals suitable for X-ray diffraction analysis of palladium complexes 1 and 2 were obtained by the slow evaporation of their acetonitrile solutions over a period of several days. The crystal structures, visualized using MERCURY software, are shown in Figure 3, while crystallographic data, including key bond lengths and angles, are listed in Tables 2 and 3.

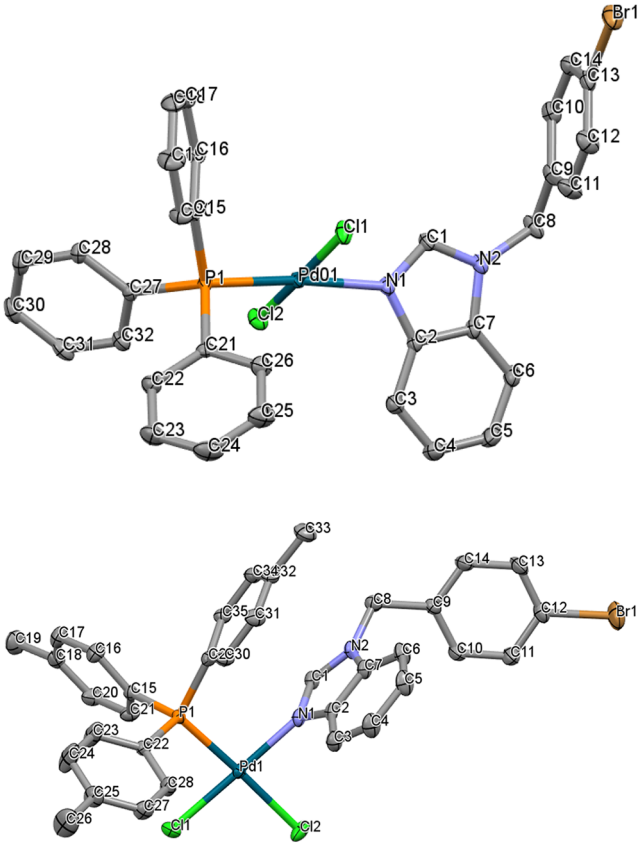

Figure 3. Crystal structure for Palladium complex 1 and 2 showing 20% probability displacement ellipsoids and atom numbering scheme.

X-ray crystallographic analysis and spectral data were found to be consistent with the proposed molecular structures of both palladium complexes 1 and 2. The molecular structures exhibit an approximately square planar geometry, with each palladium center coordinated by one nitrogen atom, one phosphorus atom, and two chloride ions as complementary anions. In complex 1, the chloride ligands occupy trans positions, whereas in complex 2, they are arranged in cis positions. The asymmetric unit of both complexes contains one phosphine ligand, one benzimidazole ligand, and two chloride atoms. The ligands coordinate to the metal center in a monodentate fashion. Both complexes crystallize in the triclinic crystal system with the P-1 space group. The longest metal−ligand bond distances were observed for the complementary chloride ions, averaging around 2.29 Å, while the shortest bonds were formed by the nitrogen atoms, with an average length of approximately 2.05 Å. Additionally, the bond angles between the central palladium atom and donor atoms were found to range between 86.965(0)° and 95.640(2)°.

3.4. Biological Activity. *3.4.1. In Vitro Ferrous Ion-Chelating Activity.* The ferrous ion-chelating capacities of the synthesized palladium(II) complexes were evaluated to assess their ability to bind transition metal ions and thus prevent Fenton-type radical generation. The chelation results, expressed as percentage inhibition of the Fe^{2+}−ferrozine complex formation, are summarized in Table 4, alongside EDTA as the reference standard.

The ferrous ion-chelating activities of Palladium complexes 1 and 2 are presented in Table 4. Complex 1 exhibited substantial chelating capacity, with 71.91% inhibition, whereas complex 2 demonstrated significantly lower activity (16.89%). These findings suggest that structural differences between the two complexes, particularly the nature of the phosphine ligands, play a key role in metal ion binding efficiency. The higher activity observed in complex 1 may be attributed to the electronic and steric environment created by the triphenylphosphine ligand, which potentially facilitates stronger coordination interactions with Fe^{2+} ions. In contrast, the presence of electron-donating methoxy groups in complex 2 might interfere with optimal metal-binding geometry. For comparison, EDTA, a well-established metal chelator, showed the highest activity (94.85%), serving as a positive control.

Notably, although Pd(II) complexes have been extensively studied for their radical scavenging properties, very limited data are available regarding their ferrous ion-chelating capabilities. Therefore, the current findings provide one of the first insights into Pd−ligand frameworks evaluated by this assay. The results support the notion that appropriately tuned Pd−ligand scaffolds may exhibit functional antioxidant properties via metal chelation, which can be valuable in therapeutic strategies targeting oxidative stress-related pathologies.

3.4.2. In Vitro Reducing Power. The reducing power of palladium(II) complexes was assessed as an indicator of their electron-donating capacity, which reflects potential antioxidant activity. The EC_{50} values, representing the concentration required to reach an absorbance of 0.5 at 700 nm, are summarized in Table 5 along with those of standard antioxidants BHT and ascorbic acid.

As shown in Table 5, palladium complex 2 exhibited stronger reducing power (EC_{50} = 1.06 ± 0.10 mg/mL) than complex 1 (EC_{50} = 1.7 ± 0.01 mg/mL), suggesting a greater electron-donating capacity. This difference may be attributed to the electron-donating methoxy groups present in the phosphine ligand of palladium complex 2, which may enhance the overall electron density of the metal center and facilitate redox interactions. Nevertheless, both complexes were less active than the reference standards BHT and ascorbic acid, as is common for metal-based antioxidants.

Reports on the reducing power of Pd(II) mononuclear complexes via FRAP-like assays are rare. One study evaluating Pd/C−SO_3H nanoparticles (a composite carbon-supported Pd system) showed EC_{50} values around 0.2 mg/mL in ferricyanide reduction assays—strongly comparable to BHT.[65,66] While nanoparticle-based systems often benefit from higher surface area and different redox dynamics, the moderate reducing capacity observed in complexes 3 and 6 remains noteworthy given their discrete coordination environment. These results highlight the impact of ligand design on Pd-based redox behavior and underscore the potential of finely tuned Pd−phosphine−benzimidazole frameworks in antioxidant development.

https://doi.org/10.1021/acsomega.5c04508
ACS Omega XXXX, XXX, XXX−XXX

Table 2. Crystal Data and Structure Refinement for Palladium Complex 1 And 2

palladium complex 1		palladium complex 2	
CCDC Number:	2473655	2473693	
empirical formula	$C_{32}H_{26}BrCl_2N_2PPd$	empirical formula	$C_{35}H_{32}BrCl_2N_2PPd$
eormula weight	726.73	formula weight	768.80
temperature/K	297.11	temperature/K	297.11
crystal system	triclinic	crystal system	triclinic
space group	*P*-1	space group	*P*-1
a/Å	9.1782(4)	*a*/Å	10.404(8)
b/Å	10.6690(5)	*b*/Å	11.389(7)
c/Å	15.5288(8)	*c*/Å	15.171(10)
α/°	92.870(2)	*α*/°	74.35(3)
β/°	97.545(2)	*β*/°	75.69(3)
γ/°	94.283(2)	*γ*/°	89.94(3)
volume/Å^3	1500.48(12)	volume/Å^3	1673(2)
Z	2	*Z*	2
ρ_{calc} g/cm^3	1.608	ρ_{calc} g/cm^3	1.526
μ/mm^{-1}	2.206	μ/mm^{-1}	1.983
F(000)	724.0	*F*(000)	772.0
crystal size/mm^3	0.1 × 0.1 × 0.1	crystal size/mm^3	0.2 × 0.15 × 0.15
radiation	Mo Kα (λ = 0.71073)	radiation	Mo Kα (λ = 0.71073)
2Θ range for data collection/°	6.092 to 56.632	2Θ range for data collection/°	6142 to 57.412
index ranges	$-12 < h < 12, -14 < k < 14, -20 < l < 20$	index ranges	$-13 < h < 13, -15 < k < 15, -20 < l < 20$
reflections collected	68597	reflections collected	47489
independent reflections	7461 [R_{int} = 0.0491, R_{sigma} = 0.0228]	independent reflections	8416 [R_{int} = 0.0399, R_{sigma}= 0.0278]
data/restraints/parameters	7461/0/353	data/restraints/parameters	8416/0/383
goodness-of-fit on F^2	1.030	goodness-of-fit on F^2	1.021
final *R* indexes [I ≥ 2σ (I)]	R_1 = 0.0259, wR_2 = 0.0580	final *R* indexes [I ≥ 2σ (I)]	R_1= 0.0290, wR_2 = 0.0647
final *R* indexes [all data]	R_1 = 0.0317, wR_2 = 0.0602	final *R* indexes [all data]	R_1 = 0.0416, wR_2 = 0.0698
largest diff. pealc/hole/e Å^{-3}	0.67/−1.01	largest diff. peak/hole/e Å^{-3}	0.60/−0.55

Table 3. Selected Bond Distances (Å) and angles (°) for Palladium Complex 1 and 2

palladium complex 1	
Bond Lengths (Å)	
Pd(1)−Cl(1)	2.2919(5)
Pd(1)−Cl(2)	2.2892(5)
Pd(1)−P(1)	2.2629(5)
Pd(1)−N(1)	2.0866(2)
Bond Angles (°)	
P(1)−Pd(1)−Cl(1)	89.441(2)
P(1)−Pd(1)−Cl(2)	95.640(2)
N(1)−Pd(1)−Cl(1)	88.270(5)
N(1)−Pd(1)−Cl(2)	87.240(5)
palladium complex 2	
Bond Lengths (Å)	
Pd(1)−Cl(1)	2.293(0)
Pd(1)−Cl(2)	2.354(0)
Pd(1)−P(1)	2.248(0)
Pd(1)−N(1)	2.036(0)
Bond Angles (°)	
P(1)−Pd(1)−Cl(1)	86.965(0)
Cl(1)−Pd(1)−Cl(2)	91.113(0)
Cl(2)−Pd(1)−N(1)	89.318(0)
N(1)−Pd(1)−P(1)	92.629(0)

3.4.3. In Vitro ABTS$^{\bullet+}$ Decolorization Assay. The ABTS$^{\bullet+}$ radical cation decolorization assay was employed to evaluate the free radical scavenging potential of the synthesized palladium(II) complexes. Percent inhibition values, representing antioxidant activity, are presented in Table 6 and compared with standard antioxidants BHT and ascorbic acid.

Table 4. Ferrous Ion-Chelating Activity Results of the Pd Complexes 1 and 2

Pd complexes	antioxidant activity (% inhibition)
palladium complex 1	71.91 ± 0.35
palladium complex 2	16.89 ± 0.36
EDTA	94.85 ± 0.49

Table 5. Reducing Power Measurement of Pd Complexes 1 and 2 Compounds

Pd complexes	EC_{50} (mg/mL)
palladium complex 1	1.7 ± 0.01
palladium complex 2	1.06 ± 0.1
BHT	0.15 ± 0.01
ascorbic acid	0.1 ± 0.01

Palladium complex 2 exhibited the highest ABTS$^{\bullet+}$ radical scavenging activity among the tested samples, even outperforming the synthetic antioxidant BHT. This enhanced

Table 6. ABTS % Inhibition Results of Palladium(II) Complexes and Standards

Pd complexes	% inhibition
palladium complex 1	49.79 ± 0.1
palladium complex 2	68.56 ± 5.01
BHT	43.55 ± 1.3
ascorbic acid	96.56 ± 0.5

https://doi.org/10.1021/acsomega.5c04508
ACS Omega XXXX, XXX, XXX−XXX

Table 7. Antiangiogenic Activity Scores of Palladium(II) Complexes and Control Samples in the CAM Assay[a]

sample	concentration (mg/pellet)	average score (mean ± SD)	antiangiogenic effect	irritation/toxicity (%)
palladium complex 1	50	0.90 ± 0.20	strong	-
palladium complex 2	50	0.85 ± 0.20	strong	-
(±)-thalidomide	50	0.90 ± 0.10	strong	-
SDS (negative ctrl)	50	-	-	84.3 ± 0.02
agar (blank)	2.5% (w/v)	-	inactive	-

[a]Values are mean of average score ± standard deviation (n = 15 for Pd complexes and n = 10 for standards). $P < 0.05$ compared with (±)-Thalidomide as positive control.

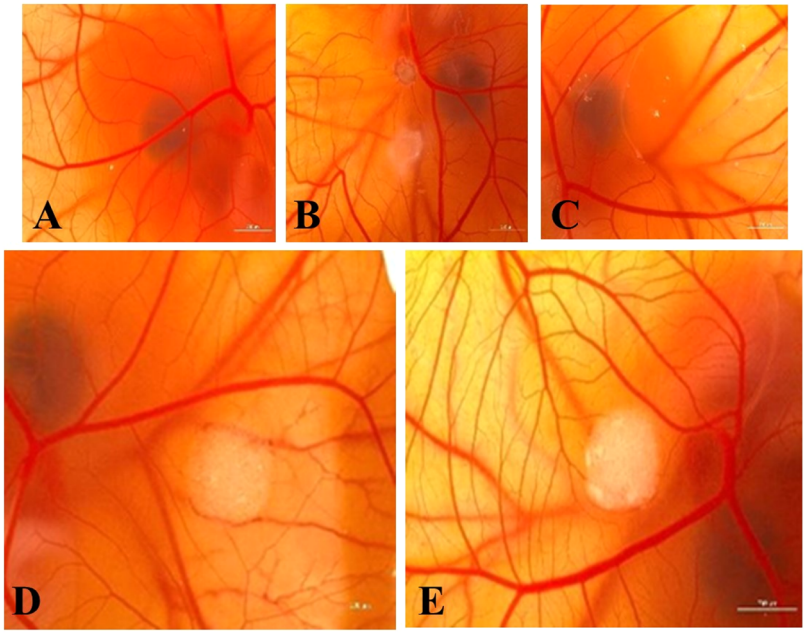

Figure 4. *In vivo* antiangiogenic effects of Pd complexes on CAM: (A) Normal embryo development with Agar (2.5%, w/v); (B) Irritant and inflammatory effect of SDS (50 μg/pellet); (C) (±)-Strong antiangiogenic effect of thalidomide (50 μg/pellet, 0.9 ± 0.1); (D) Strong antiangiogenic effect of complex 1 (50 μg/pellet, 0.90 ± 0.20); (E) Strong antiangiogenic effect of complex 2 (50 μg/pellet, 0.85 ± 0.20).

activity may be attributed to the presence of electron-donating methyl or methoxy substituents on the phosphine ligand, which likely increase the electron density around the palladium center and facilitate more effective radical quenching. In contrast, Palladium complex 1, bearing less electron-rich phosphine ligands, showed comparatively lower activity (49.79%), although still stronger than BHT (43.55%). Both complexes, however, were less active than ascorbic acid, a potent natural antioxidant.

Comparable studies on Pd−bis(benzimidazol-2-ylidene) complexes report ABTS scavenging activities in the range of 40−60%, depending on the ligand architecture and substituent electronics. Against this backdrop,[67] complex 2 demonstrates relatively higher ABTS scavenging efficiency, reinforcing the conclusion that both the benzimidazole backbone and phosphine ligand tuning are critical for optimizing antioxidant performance. These findings underline the importance of ligand electronic effects in modulating the antioxidant behavior of palladium(II) complexes and suggest that rational design of Pd−phosphine−benzimidazole frameworks can yield highly effective antioxidant agents.

3.5. *In Vivo* Angiogenic Activity (CAM Assay). *3.5.1. In Vivo Chick Embryo Chorioallantoic Membrane (CAM) assay.* The antiangiogenic activity of palladium(II) complexes 1 and 2 was evaluated using the chick chorioallantoic membrane (CAM) assay, and the results are summarized in Table 7. The scoring system was based on capillary regression around the pellet site, with higher average scores indicating stronger inhibition of angiogenesis. Representative images of vascular responses observed on the CAM are provided in Figure 4. Both complexes exhibited strong antiangiogenic effects comparable to the positive control (±)-thalidomide.

Both Pd complexes demonstrated strong inhibition of neovascularization, with average scores above 0.85. These results were comparable to the positive control, (±)-thalidomide, suggesting that the tested compounds significantly suppressed angiogenesis *in vivo*. Importantly, no irritation or toxicity was observed in embryos treated with either complex. In contrast, SDS, used as a negative control, induced substantial irritation (84.3 ± 0.02%), thereby confirming the reliability and sensitivity of the CAM assay system.

The observed antiangiogenic effects may be attributed to the interaction of the complexes with endothelial signaling pathways, potentially through redox-related mechanisms or ligand-induced molecular modulation. This is in agreement with previous studies on organometallic compounds bearing phosphine and benzimidazole ligands. The superior antioxidant and antiangiogenic activities of complex 2 may be explained by the presence of electron-donating methyl or methoxy groups on the phosphine ligand, which increase electron density at the palladium center. This enhanced electron richness likely facilitates more efficient radical

https://doi.org/10.1021/acsomega.5c04508
ACS Omega XXXX, XXX, XXX−XXX

scavenging and contributes to improved biological performance. Similar trends have been reported in the literature, where electron-rich palladium complexes exhibited enhanced bioactivity due to improved donor characteristics.[68,69]

4. CONCLUSIONS

In this study, two novel palladium(II) complexes (complex 1 and 2) incorporating phosphine and benzimidazole ligands were synthesized and structurally characterized by spectroscopic and elemental analysis techniques. Their biological activities were comprehensively assessed using *in vitro* (ferrous ion chelation, reducing power, $ABTS^{\bullet+}$ decolorization) and *in vivo* (CAM assay) models to evaluate antioxidant and antiangiogenic potential.

Both complexes demonstrated notable biological activity; however, Complex 1 exhibited the highest ferrous ion-chelating ability (71.91 ± 0.35%), while complex 2 showed the strongest $ABTS^{\bullet+}$ scavenging activity (68.56 ± 5.01%) and a relatively lower EC_{50} in reducing power assay (1.06 ± 0.1 mg/mL), indicating enhanced electron transfer capacity. *In vivo*, both complexes exhibited strong antiangiogenic effects, with average CAM assay scores (0.9 and 0.85, respectively) comparable to (±)-thalidomide, and without observable irritation or embryotoxicity.

Although both palladium(II) complexes demonstrated promising dual biological activity, complex 2 exhibited superior radical scavenging and reducing power, while Complex 1 showed stronger metal chelation capacity and slightly higher antiangiogenic scoring. These complementary strengths suggest that ligand modifications play a crucial role in modulating bioactivity, and that both compounds may serve as valuable scaffolds for future redox-targeted antiangiogenic drug development.

To the best of our knowledge, this is the first report describing the dual antioxidant and antiangiogenic activities of palladium−phosphine−benzimidazole complexes. These findings highlight the therapeutic potential of such organometallic structures as redox-modulating antiangiogenic candidates. However, it should be noted that the number of tested compounds in this study was limited, and further investigations involving a broader range of Pd(II) complexes are warranted to validate and extend these findings.Future studies should aim to clarify their underlying mechanisms, perform cellular-level validations, and investigate their pharmacokinetic profiles to determine their suitability for further drug development targeting oxidative stress−induced angiogenesis.

■ ASSOCIATED CONTENT

Supporting Information

The Supporting Information is available free of charge at https://pubs.acs.org/doi/10.1021/acsomega.5c04508.

Datablock: mo_unver_1048_0m_a (PDF)

Datablock: unver_1049_t_a (PDF)

Figure S1: FT-IR spectra of Benzimidazole ligand (page 1); Figure S2: ^{1}H-NMR spectra of Benzimidazole ligand (page 2); Figure S3: ^{13}C-NMR spectra of Benzimidazole ligand (page 2); Figure S4: FT-IR spectra of Palladium complex-1 (page 3); Figure S5: ^{1}H-NMR spectra of Palladium complex-1 (page 3); Figure S6: ^{13}C-NMR spectra of Palladium complex-1 (page 4); Figure S7: FT-IR spectra of Palladium complex-2 (page 4); Figure S8: ^{1}H-NMR spectra of Palladium complex-2 (page 5); Figure S9: ^{13}C-NMR spectra of Palladıım complex-2 (page 5) (PDF)

■ AUTHOR INFORMATION

Corresponding Author

Kübra Ögüt − *Anadolu University, Faculty of Pharmacy, Department of Pharmacognosy, 26470 Eskişehir, Türkiye*; orcid.org/0000-0002-9921-5866; Email: kubraogut@anadolu.edu.tr

Authors

Hülya Tuba Kiyan − *Anadolu University, Faculty of Pharmacy, Department of Pharmacognosy, 26470 Eskişehir, Türkiye*; orcid.org/0000-0001-5304-868X

Pervin Soyer − *Anadolu University, Faculty of Pharmacy, Department of Pharmaceutical Microbiology, 26470 Eskişehir, Türkiye*

Hakan Ünver − *Eskişehir Technical University, Faculty of Science, Department of Chemistry, 26555 Eskişehir, Türkiye*

Deniz Erol Kutucu − *Istanbul University, Faculty of Science, Department of Biology, 34134 Istanbul, Türkiye*; orcid.org/0000-0001-6867-2362

Complete contact information is available at: https://pubs.acs.org/10.1021/acsomega.5c04508

Funding

This work was financially supported by the Anadolu University Scientific Research Projects Commission under Grant No. 1907S135.

Notes

Statistical Analysis: All experiments were conducted in triplicate, and data are presented as mean ± standard deviation (SD). Statistical analysis and graphical plotting were performed using SigmaPlot software (version 15.0). Differences between groups were evaluated using one-way analysis of variance (ANOVA), followed by Tukey's posthoc test where applicable. A *p*-value of less than 0.05 was considered statistically significant.

The authors declare no competing financial interest.

■ ACKNOWLEDGMENTS

The authors gratefully acknowledge the financial support provided by the Anadolu University Scientific Research Projects Commission (BAP). The authors also acknowledge the Scientific and Technological Research Application and Research Center, Sinop University, Türkiye for the use of the Bruker D8 QUEST diffractometer.

■ REFERENCES

(1) Carmeliet, P.; Jain, R. K. Angiogenesis in Cancer and Other Diseases. *Nature* **2000**, *407* (6801), 249−257.

(2) Tahergorabi, Z.; Khazaei, M. A Review on Angiogenesis and Its Assays. *Iran. J. Basic Med. Sci.* **2012**, *15* (6), 1110−1126.

(3) Majnooni, M. B.; Fakhri, S.; Ghanadian, S. M.; Bahrami, G.; Mansouri, K.; Iranpanah, A.; Farzaei, M. H.; Mojarrab, M. Inhibiting Angiogenesis by Anti-Cancer Saponins: From Phytochemistry to Cellular Signaling Pathways. *Metabolites* **2023**, *13* (3), No. 323.

(4) Natale, G.; Bocci, G. Discovery and Development of Tumor Angiogenesis Assays. In *Tumor Angiogenesis Assays: Methods and Protocols*; Springer, 2022; pp 1−37.

(5) Yurtdaş-Kırımlıoğlu, G.; Güleç, K.; Görgülü, Ş.; Kıyan, H. T. Oseltamivir Phosphate Loaded Pegylated-Eudragit Nanoparticles for Lung Cancer Therapy: Characterization, Prolonged Release,

https://doi.org/10.1021/acsomega.5c04508
ACS Omega XXXX, XXX, XXX−XXX

Cytotoxicity Profile, Apoptosis Pathways and *in vivo* Anti-Angiogenic Effect by Using CAM Assay. *Microvasc. Res.* **2022**, *139*, No. 104251.
(6) Miklášová, N.; Fischer-Fodor, E.; Lönnecke, P.; Schrepler, M. P.; Virag, P.; Tatomir, C.; Cernea, V. I.; Hey-Hawkins, E.; Silaghi-Dumitrescu, L. Antiproliferative Effect and Genotoxicity of Novel Synthesized Palladium Complexes with Organoarsenic Ligands. *J. Inorg. Biochem* **2009**, *103* (12), 1739−1747.
(7) Waziri, I.; Yusuf, T. L.; Zarma, H. A.; Oselusi, S. O.; Coetzee, L.-C. C.; Adeyinka, A. S. New Palladium (II) Complexes from Halogen Substituted Schiff Base Ligands: Synthesis, Spectroscopic, Biological Activity, Density Functional Theory, and Molecular Docking Investigations. *Inorg. Chim. Acta* **2023**, *552*, No. 121505.
(8) Teng, Q.; Liu, W.; Zhao, Y.; Zhang, L.; Jin, H.; Meng, Q.; Frison, G. N-Heterocyclic Carbene (NHC) Ligand Exchange of Bis (NHC)−Pd (II) Complexes. *Inorg. Chem.* **2024**, *63* (46), 21806−21809.
(9) Jakovljevic, S.; Canovic, P.; Spasic, M.; Zivkovic, M.; Zaric, M.; Zaric, R. Z.; Franich, A.; Rajkovic, S.; Todorovic, Z.; Relic, N.; et al. DNA/BSA Binding Affinity and Cytotoxicity of Dinuclear Palladium (II) Complexes with Amino Acids as Ligands. *Molecules* **2025**, *30* (7), No. 1534.
(10) Hildebrandt, J.; Häfner, N.; Görls, H.; Barth, M.-C.; Dürst, M.; Runnebaum, I. B.; Weigand, W. Novel Nickel (II), Palladium (II), and Platinum (II) Complexes with O, S Bidendate Cinnamic Acid Ester Derivatives: An *in Vitro* Cytotoxic Comparison to Ruthenium (II) and Osmium (II) Analogues. *Int. J. Mol. Sci.* **2022**, *23* (12), No. 6669.
(11) Mandal, S.; Tarai, S. K.; Pan, A.; Bhaduri, R.; Biswas, P.; Moi, S. C. Cytotoxic Effects of Pd (II) Complexes on Cancer and Normal Cells: Their DNA & BSA Adduct Formation and Theoretical Approaches. *Bioorg. Chem.* **2022**, *128*, No. 106093.
(12) Darabi, F.; Hadadzadeh, H.; Simpson, J.; Shahpiri, A. A. Water-Soluble Pd (II) Complex with a Terpyridine Ligand: Experimental and Molecular Modeling Studies of the Interaction with DNA and BSA; and *in vitro* Cytotoxicity Investigations against Five Human Cancer Cell Lines. *New J. Chem.* **2016**, *40* (11), 9081−9097.
(13) Wang, X.; Guo, Z. Targeting and Delivery of Platinum-Based Anticancer Drugs. *Chem. Soc. Rev.* **2013**, *42* (1), 202−224.
(14) Kapdi, A. R.; Fairlamb, I. J. S. Anti-Cancer Palladium Complexes: A Focus on PdX 2 L 2, Palladacycles and Related Complexes. *Chem. Soc. Rev.* **2014**, *43* (13), 4751−4777.
(15) Divsalar, A.; Saboury, A. A.; Yousefi, R.; Moosavi-Movahedi, A. A.; Mansoori-Torshizi, H. Spectroscopic and Cytotoxic Studies of the Novel Designed Palladium (II) Complexes: β-Lactoglobulin and K562 as the Targets. *Int. J. Biol. Macromol.* **2007**, *40* (4), 381−386.
(16) Ulukaya, E.; Ari, F.; Dimas, K.; Sarimahmut, M.; Guney, E.; Sakellaridis, N.; Yilmaz, V. T. Cell Death-Inducing Effect of Novel Palladium (II) and Platinum (II) Complexes on Non-Small Cell Lung Cancer Cells *in vitro*. *J. Cancer Res. Clin. Oncol.* **2011**, *137*, 1425−1434.
(17) İcsel, C. DNA/HSA Interactions and Anticancer Activity of a Palladium (II) Saccharinate Complex Bearing Ethyldiphenylphosphine. *Hacettepe J. Biol. Chem.* **2021**, *49* (1), 107−116.
(18) Kacar, O.; Adiguzel, Z.; Yilmaz, V. T.; Cetin, Y.; Cevatemre, B.; Arda, N.; Baykal, A. T.; Ulukaya, E.; Acilan, C. Evaluation of the Molecular Mechanisms of a Palladium (II) Saccharinate Complex with Terpyridine as an Anticancer Agent. *Anticancer Drugs* **2014**, *25* (1), 17−29.
(19) Savić, A.; Marzo, T.; Scaletti, F.; Massai, L.; Bartoli, G.; Hoogenboom, R.; Messori, L.; Van Deun, R.; Van Hecke, K. New Platinum (II) and Palladium (II) Complexes with Substituted Terpyridine Ligands: Synthesis and Characterization, Cytotoxicity and Reactivity towards Biomolecules. *BioMetals* **2019**, *32*, 33−47.
(20) Hassan, S. S.; Hosny, W. M.; Aboutabl, M. A.; Fayed, D. B.; Khalf-Alla, P. A. Comparison of *In Vitro* and *In Vivo* Biological Screening of Nano-Palladium (II) and Platinum (II)-Based Compounds With DFT and Molecular Docking Study. *Appl. Organomet. Chem.* **2024**, *38* (12), No. e7713.
(21) Rayasingh, A. R.; Manivannan, V. Palladium (Ii) and Platinum (Ii) Complexes of Disubstituted Imidazo [1, 5-a] Pyridine and Imidazolylpyridine: Coordination Chemistry, Versatile Catalysis, and Biophysical Study. *Dalton Trans.* **2025**, *54* (19), 7741−7752.
(22) Yang, F.; Wei, P.; Yang, M.; Chen, W.; Zhao, B.; Li, W.; Wang, J.; Qiu, L.; Chen, J. Redox-Sensitive Hyaluronic Acid-Ferrocene Micelles Delivering Doxorubicin for Enhanced Tumor Treatment by Synergistic Chemo/Chemodynamic Therepay. *J. Drug Delivery Sci. Technol.* **2022**, *77*, No. 103851.
(23) Tarai, S. K.; Pan, A.; Biswas, P.; Bhaduri, R.; Mandal, S.; Paul, A.; Baitalik, S.; Bhattacharjee, A.; Moi, S. C. Anticancer Behavior of Pyrrolidine-Based Palladium (II) Complexes and Biophysical Approach on Their DNA, BSA Binding Activity, Molecular Docking, and DFT Study. *Langmuir* **2023**, *39* (31), 10947−10964.
(24) Abu-Dief, A. M.; Said, M. A.; Elhady, O.; Alahmadi, N.; Alzahrani, S.; Eskander, T. N. A.; Ali, M. A. E. A. A. Designing of Some Novel Pd (II), Ni (II) and Fe (III) Complexes: Synthesis, Structural Elucidation, Biomedical Applications, DFT and Docking Approaches against Covid-19. *Inorg. Chem. Commun.* **2023**, *155*, No. 110955.
(25) Romashev, N. F.; Abramov, P. A.; Bakaev, I. V.; Fomenko, I. S.; Samsonenko, D. G.; Novikov, A. S.; Tong, K. K. H.; Ahn, D.; Dorovatovskii, P. V.; Zubavichus, Y. V.; et al. Heteroleptic Pd (II) and Pt (II) Complexes with Redox-Active Ligands: Synthesis, Structure, and Multimodal Anticancer Mechanism. *Inorg. Chem.* **2022**, *61* (4), 2105−2118.
(26) Al-Fakeh, M. S.; Alsikhan, M. A.; Alnawmasi, J. S. Physico-Chemical Study of Mn (II), Co (II), Cu (II), Cr (III), and Pd (II) Complexes with Schiff-Base and Aminopyrimidyl Derivatives and Anti-Cancer, Antioxidant, Antimicrobial Applications. *Molecules* **2023**, *28* (6), No. 2555.
(27) Pruchnik, H.; Solarska-Ściuk, K.; Dudek, A.; Włoch, A. Impact of a Palladium (II)-Tris (2-Carboxyethyl) Phosphine Complex on Normal Cells: Toxicity and Membrane Interaction. *Molecules* **2025**, *30* (3), No. 476.
(28) Ndagi, U.; Mhlongo, N.; Soliman, M. E. Metal Complexes in Cancer Therapy−an Update from Drug Design Perspective. *Drug Des., Dev. Ther.* **2017**, *11*, 599−616.
(29) Gasser, G.; Ott, I.; Metzler-Nolte, N. Organometallic Anticancer Compounds. *J. Med. Chem.* **2011**, *54* (1), 3−25.
(30) Demir, B. S.; Keleş, T.; Serindağ, O. Antioxidant Enzyme Inhibitor Role of Phosphine Metal Complexes in Lung and Leukemia Cell Lines. *Bioinorg. Chem. Appl.* **2014**, *2014* (1), No. 717421.
(31) Bagowski, C. P.; You, Y.; Scheffler, H.; Vlecken, D. H.; Schmitz, D. J.; Ott, I. Naphthalimide Gold (I) Phosphine Complexes as Anticancer Metallodrugs. *Dalton Trans.* **2009**, No. 48, 10799−10805.
(32) Reddy, T. S.; Privér, S. H.; Mirzadeh, N.; Bhargava, S. K. Synthesis of Gold (I) Phosphine Complexes Containing the 2-BrC6F4PPh2 Ligand: Evaluation of Anticancer Activity in 2D and 3D Spheroidal Models of HeLa Cancer Cells. *Eur. J. Med. Chem.* **2018**, *145*, 291−301.
(33) El Rashedy, A. A.; Aboul-Enein, H. Y. Benzimidazole Derivatives as Potential Anticancer Agents. *Mini Rev. Med. Chem.* **2013**, *13* (3), 399−407.
(34) Shrivastava, N.; Naim, M. J.; Alam, M. J.; Nawaz, F.; Ahmed, S.; Alam, O. Benzimidazole Scaffold as Anticancer Agent: Synthetic Approaches and Structure−Activity Relationship. *Arch. Pharm.* **2017**, *350* (6), No. e201700040.
(35) Çevik, U. A.; Kaya, B.; Celik, I.; Rudrapal, M.; Rakshit, G.; Karayel, A.; Levent, S.; Osmaniye, D.; Sağlık Özkan, B. N.; Baysal, M.; et al. New Benzimidazole-Triazole Derivatives as Topoisomerase i Inhibitors: Design, Synthesis, Anticancer Screening, and Molecular Modeling Studies. *ACS Omega* **2024**, *9* (11), 13359−13372.
(36) Kıyan, H. T.; Öztürk, N.; Poyraz, İ. E. Total Phenolic Content and Biological Activities of *Gentiana pyrenaica* L. *Free Radicals Biol. Med.* **2016**, *100*, No. S102.
(37) Kıyan, H. T.; Demirci, B.; Başer, K. H. C.; Demirci, F. The *in vivo* Evaluation of Anti-Angiogenic Effects of *Hypericum* Essential Oils Using the Chorioallantoic Membrane Assay. *Pharm. Biol.* **2014**, *52* (1), 44−50.

https://doi.org/10.1021/acsomega.5c04508
ACS Omega XXXX, XXX, XXX−XXX

(38) Ikitimur-Armutak, E. I.; Gurel-Gurevin, E.; Kiyan, H. T.; Aydinlik, S.; Yilmaz, V. T.; Dimas, K.; Ulukaya, E. Anti-Angiogenic Effect of a Palladium (II)-Saccharinate Complex of Terpyridine *in vitro* and *in vivo*. *Microvasc. Res.* **2017**, *109*, 26−33.
(39) Alessio, E. *Bioinorganic Medicinal Chemistry*; John Wiley & Sons, 2011.
(40) Czarnomysy, R.; Radomska, D.; Szewczyk, O. K.; Roszczenko, P.; Bielawski, K. Platinum and Palladium Complexes as Promising Sources for Antitumor Treatments. *Int. J. Mol. Sci.* **2021**, *22* (15), No. 8271.
(41) Mahmood, K.; Akhter, Z.; Perveen, F.; Bibi, M.; Ismail, H.; Tabassum, N.; Yousuf, S.; Ashraf, A. R.; Qayyum, M. A.; Aisha. Synthesis, DNA Binding and Biological Evaluation of Benzimidazole Schiff Base Ligands and Their Metal (II) Complexes. *RSC Adv.* **2023**, *13* (18), 11982−11999.
(42) Naziruddin, A. R.; Hepp, A.; Pape, T.; Hahn, F. E. Synthesis of Rhodium (i) Complexes Bearing Bidentate NH, NR-NHC/Phosphine Ligands. *Organometallics* **2011**, *30* (21), 5859−5866.
(43) Shawky, H.; Fayed, D. B.; Ibrahim, N. E. PH-Tailored Delivery of a Multitarget Anticancer Benzimidazole Derivative Using a PEGylated β-Cyclodextrin-Curcumin Functionalized Nanocomplex. *Biomater. Adv.* **2024**, *163*, No. 213964.
(44) Venter, J. A.; Purcell, W.; Visser, H. G. Di-μ-Iodido-Bis [Acetyl (4-Methyl-2, 6, 7-Trioxa-1-Phosphabicyclo [2.2. 2] Octane)(N-Nitroso-N-Oxidoaniline-K2O, O′) Rhodium (III)]. *Struct. Rep.* **2009**, *65* (12), m1528−m1529.
(45) Dolomanov, O. V.; Bourhis, L. J.; Gildea, R. J.; Howard, J. A. K.; Puschmann, H. OLEX2: A Complete Structure Solution, Refinement and Analysis Program. *Appl. Crystallogr.* **2009**, *42* (2), 339−341.
(46) Sheldrick, G. M. SHELXT−Integrated Space-Group and Crystal-Structure Determination. *Acta Crystallogr., Sect. A:Found. Adv.* **2015**, *71* (1), 3−8.
(47) Macrae, C. F.; Edgington, P. R.; McCabe, P.; Pidcock, E.; Shields, G. P.; Taylor, R.; Towler, M.; Streek, J. V. D. Mercury: Visualization and Analysis of Crystal Structures. *J. Appl. Crystallogr.* **2006**, *39* (3), 453−457.
(48) Gao, G.; Xia, H.; Shi, J.; Zheng, P.; Wu, W.; Wu, S.; Qi, T.; Song, H.; Gu, Y.; Li, J.; et al. Carbon Dot Nanozymes with Ferrous Ion-Chelating and Antioxidative Activity Inhibiting Ferroptosis to Alleviate Renal Ischemia-Reperfusion Injury. *Small* **2025**, *21* (16), No. 2407372.
(49) Khan, M.; Raheel, M.; Shah, S.; Ibrahim, M.; Asif, M.; Salar, U.; Khan, K. M. Synthesis, Characterization, DPPH, Ferric Reducing, and Ferrous Ion-Chelating Activities of Isophthalate Schiff Bases. *Lett. Drug Des. Discovery* **2023**, *20* (1), 31−39.
(50) Orhan, I.; Üstün, O. Determination of Total Phenol Content, Antioxidant Activity and Acetylcholinesterase Inhibition in Selected Mushrooms from Turkey. *J. Food Compos. Anal.* **2011**, *24* (3), 386−390.
(51) Gulcin, İ.; Alwasel, S. H. Fe^{3+} Reducing Power as the Most Common Assay for Understanding the Biological Functions of Antioxidants. *Processes* **2025**, *13* (5), No. 1296.
(52) Vijayalakshmi, M.; Ruckmani, K. Ferric Reducing Antioxidant Power Assay in Plant Extract. *Bangladesh J. Pharmacol.* **2016**, *11* (3), 570−572.
(53) Lee, Y.-L.; Yen, M.-T.; Mau, J.-L. Antioxidant Properties of Various Extracts from *Hypsizigus marmoreus*. *Food Chem.* **2007**, *104* (1), 1−9.
(54) Ögüt, K.; Özek, G.; Öztürk, N.; Tekin, M.; Özek, T. Comprehensive Investigation of Phytochemical Constituents and Biological Activities of *Scabiosa pseudograminifolia* Hub.-Mor. *Turk. J. Pharm. Sci.* **2025**, *22*, 104−118.
(55) Öğüt, K.; Özek, G.; Öztürk, N.; Yaylacı, Ö. K.; Özek, T. Chemical Composition, α-Amylase Inhibition, and Antioxidant Activities of *Scabiosa hololeuca* Bornm. *Biochem Syst. Ecol* **2025**, *122*, No. 105028.
(56) Gurel-Gurevin, E.; Kiyan, H. T.; Esener, O. B. B.; Aydinlik, S.; Uvez, A.; Ulukaya, E.; Dimas, K.; Armutak, E. I. Chloroquine Used in Combination with Chemotherapy Synergistically Suppresses Growth and Angiogenesis *in vitro* and *in vivo*. *Anticancer Res.* **2018**, *38* (7), 4011−4020.
(57) Yurtdaş-Kırımlıoğlu, G.; Görgülü, Ş.; Guelec, K.; Kıyan, H. T. Nanoarchitectonics of PLGA Based Polymeric Nanoparticles with Oseltamivir Phosphate for Lung Cancer Therapy: *In vitro-in vivo* Evaluation. *J. Drug Delivery Sci. Technol.* **2022**, *67*, No. 102996.
(58) Ari, F.; Cevatemre, B.; Armutak, E. I. I.; Aztopal, N.; Yilmaz, V. T.; Ulukaya, E. Apoptosis-Inducing Effect of a Palladium (II) Saccharinate Complex of Terpyridine on Human Breast Cancer Cells *in vitro* and *in vivo*. *Bioorg. Med. Chem.* **2014**, *22* (17), 4948−4954.
(59) Ikitimur-Armutak, E. I.; Gurel-Gurevin, E.; Kıyan, H. T.; Aydinlik, S.; Yilmaz, V. T.; Dimas, K.; Ulukaya, E. Anti-Angiogenic Effect of a Palladium (II)-Saccharinate Complex of Terpyridine *in vitro* and *in vivo*. *Microvasc. Res.* **2016**, *109*, 26−33.
(60) Ari, F.; Cevatemre, B.; Armutak, E. I. I.; Aztopal, N.; Yilmaz, V. T.; Ulukaya, E. Apoptosis-Inducing Effect of a Palladium (II) Saccharinate Complex of Terpyridine on Human Breast Cancer Cells *in vitro* and *in vivo*. *Bioorg. Med. Chem.* **2014**, *22*, 4948−4954.
(61) Uvez, A.; Aydinlik, S.; Esener, O. B. B.; Erkisa, M.; Karakus, D.; Armutak, E. I. Synergistic Interactions between Resveratrol and Doxorubicin Inhibit Angiogenesis Both *in vitro* and *in vivo*. *Pol. J. Vet. Sci.* **2020**, *23* (4), 571−580.
(62) Kıyan, H. T.; Üvez, A.; Erkisa, M.; Ikitimur-Armutak, E. İ.; Yılmazer, N.; Esener, O. B. B.; Kutucu, D. E.; Üstünova, S.; Ulukaya, E.; Öztürk, A. A.; Gürel-Gürevin, E. A Comparative Study on *in vitro* Anti-Cancer and *in vivo* Anti-Angiogenic Effects of TRPC Blockers Pyr-3 and SKF-96365. *Lett. Drug Des. Discovery* **2023**, *20* (7), 957−964.
(63) Aydinlik, S.; Uvez, A.; Kiyan, H. T.; Gurel-Gurevin, E.; Yilmaz, V. T.; Ulukaya, E.; Armutak, E. I. Palladium (Ii) Complex and Thalidomide Intercept Angiogenic Signaling via Targeting Fak/Src and Erk/Akt/Plcγ Dependent Autophagy Pathways in Human Umbilical Vein Endothelial Cells. *Microvasc. Res.* **2021**, *138*, No. 104229.
(64) Huan-huan, C.; Li-Li, Y.; Shang-Bin, L. Artesunate Reduces Chicken Chorioallantoic Membrane Neovascularisation and Exhibits Antiangiogenic and Apoptotic Activity on Human Microvascular Dermal Endothelial Cell. *Cancer Lett.* **2004**, *211* (2), 163−173.
(65) Zhu, H.; Ni, L.; Ren, S.; Fang, G.; Li, S. A Composite Carbon-Based Solid Acid-Supported Palladium Catalyst (Pd/C-SO 3 H) for Hydrogenolysis of Plant-Derived Polymeric Proanthocyanidins. *RSC Adv.* **2020**, *10* (35), 20665−20675.
(66) Munteanu, I. G.; Apetrei, C. Analytical Methods Used in Determining Antioxidant Activity: A Review. *Int. J. Mol. Sci.* **2021**, *22* (7), No. 3380.
(67) Amri, N.; Mukhrish, Y. E.; Özdemir, I.; Gürbüz, N.; Arfaoui, Y.; Mansour, L.; Gatri, R.; Beji, L.; Hamdi, N. From Synthesis to Biological Impact of Palladium Bis (Benzimidazol-2-Ylidene) Complexes: Preparation, Characterization, and Antimicrobial and Scavenging Activity. *Main Group Met. Chem.* **2023**, *46* (1), No. 20230007.
(68) Ezzatzadeh, E.; Soleimani-Amiri, S.; Hossaini, Z.; Khandan Barani, K. Synthesis and Evaluation of the Antioxidant Activity of New Spiro-1, 2, 4-Triazine Derivatives Applying Ag/Fe3O4/CdO@MWCNT MNCs as Efficient Organometallic Nanocatalysts. *Front. Chem.* **2022**, *10*, No. 1001707.
(69) Fadhel, A. Z.; Pollet, P.; Liotta, C. L.; Eckert, C. A. Combining the Benefits of Homogeneous and Heterogeneous Catalysis with Tunable Solvents and Nearcritical Water. *Molecules* **2010**, *15* (11), 8400−8424.

https://doi.org/10.1021/acsomega.5c04508
ACS Omega XXXX, XXX, XXX−XXX